International Journal of Membrane Science and Technology, 2023, Vol. 10, No. 2, pp 3815-3834

The Effect of Absorbed Dose and Chemical Composition On the Ionic Conductivity of 1-Vinylimidazole-Grafted Pvdf Membranes Made Via Γ-Ray Induced Grafting

A. Lepit[1*], M. Mustaffa[2], N. K. Jaafar[2], N. A. Aini[2]

[1]Faculty of Applied Sciences, Universiti Teknologi MARA Sabah Branch, Kota Kinabalu Campus, Sabah, 88997, Malaysia
[2]Faculty of Applied Sciences, Universiti Teknologi MARA, 40450 Shah Alam Selangor, Malaysia
**Correspondence email: nazli2005@uitm.edu.my , ajis@uitm.edu.my*

Abstracts: The effect of γ-ray on the copolymerization of 1-Vinylimidazole (VIm) onto polyvinyl fluoride (PVDF) is dependent on the absorbed dose, various solvents, and Iron concentration (II). Using radiation-induced grafting techniques, develop an alternative proton-exchange membrane (PEM) based on PVDF as the primary polymer and VIm as the monomer. Gravimetric analysis, FTIR, and conductivity investigation were utilized to characterize the physico-chemical properties of the grafting membrane. PEM, also known as PVDF-g-P1VIm, was synthesized and functionalized by sulfuric acid doping. The proportion of dose absorbed, the degree of grafting (DG), the ion exchange capacity (IEC), and water uptake (WU) all correlate with the membrane grafting performance. The C-H bonds exhibited decreased intensity and the peak location moved considerably in FTIR, indicating PVDF-VIm grafting. DG and IEC influence the ionic conductivity of the grafting PEM. The grafted membranes proved to have humidity dependent on proton conductivity with a range of 0.136 $\mathrm{mScm^{-1}}$ (room temperature) and 3.02 $\mathrm{mScm^{-1}}$ (373 K) containing IEC levels of 0.065 and 0.107 meq./g, respectively. PVDF-g-P1VIm membranes exhibit potential in the field of PEM membranes for use in hydrogen fuel cells or water treatment.

Keywords: Degree of Grafting, Conductivity, Γ-Ray, PVDF, 1-Vinylimidazole

1. INTRODUCTION

Today we receive carbon emissions and global warming effects from human activities through industry, construction activities, opening a new land, forest burning etc. The industry currently relies heavily on fossil fuels from petroleum as a source of energy to drive machinery, portable & stationary mechanical equipment, and transportation. Emissions of pollutants from petroleum fuels affect the rising temperature of the environment [1,2]. Therefore, the search for cleaner and more environmentally friendly fuels is still active in research and innovation to create clean energy conversion devices (ECD) [3,4]. ECD such as fuel cells, one of the devices based on hydrogen energy, is developing nowadays [5,6]. The core of a polymer electrolyte membrane in the fuel cell is the ion exchange membrane [7,8]. Furthermore, proton exchange membranes (PEM) based on Nafion are expensive, low–low-temperature PEMs, limiting their utility for high–temperature applications and commercial purposes [8,9]. PEM is essential for energy conversion, which can transform chemical energy into electricity without air pollution. Therefore, PEM based on graft copolymerization of 1-VIm onto PVDF was studied and synthesized.

PVDF is a widely investigated polymer due to its excellent mechanical properties and chemical stability with a simple chemical formula -CH2-CF2- [10]. PVDF is an attractive base polymer that has been the focus of numerous studies for many years because of its unique electrical properties, weather resistance, durability, biocompatibility, thermal stability, and excellent radiation resistance [11,12]. PEM is obtained by introducing various polar and functional monomers to PVDF films using radiation-induced graft copolymerization. Radiation-induced simultaneous grafting is a process where ionizing radiation produces scission on the weakest bond such as C-H bonds primary of the polymer and double bond in monomer with the existence of initiator and then it occurs grafting of a monomer onto the polymer. This site is usually a free radical, where the polymer chain behaves like a macroradical. Radiation technique may subsequently initiate the polymerization of a monomer, leading to the formation of a graft copolymer structure [13]. The graft copolymer, in general, can be defined as consisting of one or more molecules, as a block, connected as a side chain to the main chain. This side chain should have constitutional or configurational features that differ from the main chain's [14].

Ionizing radiation such as γ-ray and electron beams can be considered high energy penetration of radiation. It can ionize the atoms or break bonds of molecules of the materials they pass through, increasing their reactivity or ability to form new materials. The degree of damage, materials improvement, polymerization, and grafting depends upon radiation dose. For example, in electron beam processing, energetic electrons strike molecules at/or near carbon-hydrogen bonds, freeing hydrogen atoms and leaving the molecules with excited carbon atoms (radicals) at the point of impact. When this occurs at two adjacent molecules or/at nearby sites, then excited carbon atoms can release excitation energy, forming a chemical bond between pairs of polymer molecules [15]. Copolymerization can happen at the correct radiation dose to promote graft or cross-linking those spreads throughout the polymer [16,17]. Radiation-induced grafting has many advantages and applications, such as modifying the physical and chemical properties of textile fabrics [18,19], in medical implant applications using ePTFE-g-HEMA as a biomaterial [20], modifying hydrophobic PVDF to the hydrophilic membrane [21].

1-Vinylimidazole (VIm) is also known as 1-Ethenyl-1H-Imidazole. VIm has been chosen because of an essential chemical with a wide variety of uses and applications, such as the formation of polymers, complexation with cations, and corrosion inhibitors and reported that VIm could attract water by constructing bridged water (Im-H2O-Im) and metal ion (M2+). Because of the tertiary amine groups, polybase, and pH-dependent positive charge density, polyvinyl imidazole (PVI) is an interesting polymer form of VIm to work with. Additionally, PVI-containing imidazole groups was used as a model polyelectrolyte to investigate the adsorption characteristics of different minerals due to their complexation with catalytic divalent metallic ions such as Co2+ and Cu2+ [22]. Copolymerization of VIm was obtained via the comonomer effect Zor binary graft copolymers by ionizing grafting radiation using the simultaneous technique [23]. PVDF and VIm can graft via γ-ray induced grafting. γ-rays process is performed in three steps: (i) the simultaneous of the base matrix by γ-rays; (ii) the grafting of the monomer, 1-Vinylimidazole onto PVDF; (iii) and finally, the protonation of the grafted membrane by sulfuric acid [24]. Grafting occurs between primary hydrophobic polymer and hydrophilic side monomer; usually, solid thin-film polymer and monomer solution complexion with a metal salt solution such as FeCl2.6H2O, CuCl2.2H2O CoCl2.6H2O etc. as a catalytic centre [25].

Iron (II) sulfate is a class of metal chelates that activates the grafting reaction and forms a grafted copolymer that occurs at the optimum amount or molar ratio with other chemicals. An activation effect of Fe2+ chelates on the rate of polymerization is interpreted from the point of redox reactions of coordinated compounds [26]. Iron (II) sulfate also acts as a polymerization activator. For instance, grafting yield, homopolymer, and grafting efficiency depend upon the concentration of the Fe2+ ion for initiating grafting processes between monomer and polymer [27,28]. The γ-rays as high ionizing radiation can trigger –CH2 free radical through scissions from the polymer backbone and then induce the grafting, polymerization or cross-linking of vinyl monomer [29]. In addition, radiation-induced graft polymerization of acrylamide (AAm) onto poly (tetrafluoroethylene/hexafluoropropylene/vinylidene fluoride) (TFB) films was investigated using ferrous ammonium sulphate as an inhibitor to reduce acrylamide homopolymerization [30]. Hence, it is essential to use Iron (II) as a grafting initiator

This paper presents and discusses the effects of a few variable parameters such as absorption of radiation, types of solvent, catalyst concentration and monomer concentration on the properties of samples during preparation and radiation processes. The irradiation process was performed to determine the optimum concentration of monomers and different solvents with absorbed doses. As well, the concentration of ferrous was also chosen for the grafting optimum. The optimum absorption dose, type of solvent, and iron (II) concentration were then selected to be used in the final stage of sample preparation. For physical measurement, the best samples of PVDF-g-P1VIm(H+) with the best percentage value of the DG were chosen. They then measured the chemical properties of the samples via FTIR and conductivity characterization via impedance spectroscopy. Our results provide the framework for the correlation between DG, IEC, WU and conductivity properties.

2. MATERIAL AND METHODS

The irradiation method used was simultaneous irradiation. Simultaneous irradiation was a method in which the polymer and monomer solution were irradiated simultaneously containing polymer, solvent, and a monomer with and without a catalyst. Two stages of samples characterization were carried out. In the first stage, the effects of radiation dose, the different solvent types, and the presence with and without the catalyst on the physical properties of the samples were observed. In the second stage, irradiated at the best-absorbed dose of 60kGy for different concentrations of monomer and ferrous.

2.1Materials

PVDF with an average molecular weight of 400,000 gmol-1, 1-Vinylimidazole (purity ≥ 99%), acetone (purity ≥ 99.50%) and Iron (II) sulfate heptahydrate (purity ≥ 99.0%) was purchased from Sigma-Aldrich. The solvent, DMF (purity ≥ 98%) and sulfuric acid fuming (purity ≥ 65.0%), 1-Butanol (74.12 g/mol), Cyclohexane (84.16 g/mol), 1,4-Dioxane (88.11 g/mol) were purchased from Merck was used as received to prepare the samples. 1-Vinylimidazole (purity ≥ 99%), acetone (purity ≥ 99.50%) and Iron (II) sulfate heptahydrate (purity ≥ 99.0%) were purchased from Sigma-Aldrich. The solvent, DMF (purity ≥ 98%) and sulfuric acid fuming (purity ≥ 65.0%), 1-Butanol (74.12 g/mol), Cyclohexane (84.16 g/mol), 1,4-Dioxane (88.11 g/mol) were purchased from Merck was used as received to prepare the samples.

2.2 Irradiation Source and Processing

Irradiation of the sample was divided into two stages. The first stage of irradiation was conducted with different absorbed doses delivered. The number of absorbed doses given was set at 20, 40, 60, 80 and 100 kGy at MINTec-Sinagama, Nuclear Malaysia [31]. The first attempt aimed to find the best dose delivered to the samples using unstable isotope Co-60. All irradiation of the sample pieces were irradiated using a simultaneous irradiation technique in a nitrogen atmosphere. The optimum radiation dose, the best solvent used, and with or without the initiator based on the highest percentage of monomer attached to the polymer (known as gravimetric analysis) were chosen for use in the next irradiation stage. These parameters were then used as a benchmark for irradiating samples in the second stage of irradiation.

For the second attempt, simultaneous irradiation of γ-rays was carried out at a constant absorbed dose of 60 kGy since this absorbed dose was the best for grafting processing. The PVDF films in circular shape were then weighed and immersed in the 1-vinyl imidazole dissolved in different solvents (e.g., Cyclohexane, Butanol, 1,4 – dioxane) as a monomer solution at concentrations 0.5, 1.0, 2.0 and 3.0 M for 12 hours. The irradiation was carried out at a dose rate of 0.0364 kGy/min, Co-60 γ-rays at MINTec-Sinagama facilities, Malaysian Nuclear Agency. The PVDF, 1-VIm, Iron (II) and solvent were irradiated concurrently to search and verify dependent parameters.

2.3 Preparation & Synthesis of Membrane

PVDF (1.0 g) was dissolved in 12 ml DMF. The solution was stirred for 18 hours at room temperature. Once the polymer was fully dissolved, the PVDF solution was cast into a glass plate and then subsequently dried in an oven at 60oC for 5 hours. The obtained films have a thickness in the range of 20-110 µm. Then, the PVDF films were cut into a circular shape and weighed before irradiation. Then the films were immersed in the 1-vinylimidazole monomer mixed with solvent Cyclohexane, Butanol, and 1,4 – dioxane respectively, in glass bottles at concentrations ratio; VIm/solvent, 1/1 (v/v) containing 0.0025 M of $FeSO_4.7H_2O$ as a grafting initiator. The film samples were purged and kept under nitrogen gas in a sealed glass-bottled before irradiation using a γ-ray that operated at a dose rate of 0.0364 kGy/min which irradiation time took 21 hours in the constant absorbed dose of 60 kGy. After irradiation, the membrane was immersed immediately in a sulfuric acid concentration of 0.5 M for a day. Wash with distilled water three times a day and wash again with ethanol for 4 hours. Finally, the samples were dried in the oven at 70oC for 8 hrs. Two types of samples measured and reported in this paper were based on the monomer concentration and DG of the final prepared PEM.

2.4 Characterizations of Membrane

After obtaining the desired characteristics, the best samples were selected for further characterization, which included gravimetric analysis, infrared spectroscopy, and conductivity testing.

2.4.1 Degree of Grafting

The grafting of the samples was determined by the mass method. The ungrafted monomer and homopolymer were removed and firstly washed thoroughly in deionized water (12 hours), followed by methanol (12 hours) and lastly in deionized water (12 hours) with a total clean-up of 36 hours. The degree of grafting (DG) was determined using equation (1):

$$\text{Degree of Grafting } (\%) = \frac{w_g - w_i}{w_i} \times 100 \quad (1)$$

where w_g is the weight of PVDF-g-P1VIm and w_i is the weight of PVDF only.

2.4.2 Degree of Protonation

The grafted PVDF-g-P1VIm films were protonated using 0.5 M sulfuric acid at a temperature of 60°C for 2 hours and later cooled at room temperature for 12 hours. After completing the reaction, the membranes were cleaned with distilled water several times until the pH was close to 7 and then dried in the oven at 60-70°C. PVDF-g-P1VIm (H^+) is the grafting monomers with acid contained as a functional group. The degree of protonation (DP) was calculated using equation (2), where w_p and w_g are the weights of dry protonated and non-protonated grafted membranes, respectively.

$$\text{Degree of Protonation } (\%) = \frac{w_p - w_g}{w_g} \times 100 \quad (2)$$

2.4.3 Ion Exchange Capacity

The ion exchange capacity (IEC) of the prepared proton exchange membranes was determined by acid-base titration. The prepared acidic membranes (protonic form) were immersed in 0.5 M NaCl solution at room temperature (28°C) for 24 hours. The protons (H^+) released in the solution, substituted by sodium ion (Na^+) with standardized 0.012 M NaOH solution using phenolphthalein as an indicator. The IEC of the membranes was calculated using the equation (3):

$$\text{IEC}\left(\text{meq.}\frac{1}{g}\right) = \left(\frac{C_{NaOH} \times V_{NaOH}}{w_{dry}}\right) \quad (3)$$

where C_{NaOH} (molL^{-1}) and V_{NaOH} (mL) are the concentration and volume of NaOH solution required for neutralization of the residual solution, and w_{dry} is the weight of the dry protonated membrane.

2.4.4 Degree of Swelling

To determine the degree of swelling (DS), the membranes were immersed in distilled water at room temperature for 45 min. Water on the surface was mopped off the wet film with absorbent paper, and the diameter of the swollen membranes was measured immediately, and was calculated using equation (4):

$$\text{Degree of Swelling } (\%) = \frac{d_s - d_d}{d_d} \times 100 \quad (4)$$

where d_d and d_s are the dry and swollen diameters of used membranes, respectively.

2.4.5 Water Uptake

Water uptake (WU) is defined as the mass of water absorbed by the membrane divided by the dry weight, according to the equation (5):

$$\text{Water Uptake}(\%) = \frac{w_s - w_d}{w_d} \times 100 \qquad (5)$$

where w_d and w_s are the weight of the dry and wet membranes, respectively, the grafted membranes, dried to constant weight, were immersed, and stirred in distilled water at room temperature for 12 hours to attain equilibrium. Three repeat measurements were carried out for each membrane.

2.4.6 Fourier Transform Infrared Spectroscopy

Fourier transforms infrared (FTIR) spectroscopy is an analytical technique that gives information about the functional group and chemical bonds in materials through the investigation of the vibrational state of the functional group. FTIR spectroscopy analyses of the pristine PVDF, PVDF-g-P1VIm, and protonated PVDF-g-P1VIm membrane were measured using Varian 3100, Excalibur Series. The spectra of the samples were measured in the transmittance mode at a wavenumber of 4000 to 600 cm^{-1} with a resolution of 4.0 cm^{-1}. FTIR spectra of the samples were analyzed with Varian's Resolution Pro software.

2.4.7 Transference Number

The transference number of protonated membrane samples was determined using two blocking Aluminum electrodes positioned between them. A slight constant potential difference of 0.8 V was applied across the sample, and the current was measured as a function of time until it reached a constant value. The time obtained from the plot of normalized polarization current-time using the equation (6):

$$t_{ion} = 1 - \frac{I_t}{I_T} \qquad (6)$$

where I_s is the current on the steady-state condition and I_T is the total current.

2.4.8 Conductivity Measurements

The Ionics conductivity (σ) of the membrane was determined by an alternating current (AC) technique from the Cole-Cole plot. These plots were obtained using the WonATech Multichannel electrochemical impedance analyzer (WEIS510) System in the frequency range 10 Hz to 1 MH. The measurements were carried out in a controlling temperature range between 298 K and 373 K inside a Humidity & Temperature Chamber (ESPEC-SH 221) at relative humidity (RH) of 80-90%. The hydrated membranes were placed into small discs of 2.0 cm^2 size and clamped between two stainless steel electrodes. The conductivity was evaluated using the equation (7):

$$\sigma(S.cm^{-1}) = \frac{t}{R_b A} \qquad (7)$$

Where t is the thickness of the membrane (cm); A is the area of surface between electrode and membrane (cm^2); R_b is the bulk resistance of the membrane obtained from the impedance plot (Ω).

3.RESULTS AND DISCUSSION

3.1 Degree of Grafting with Variation of Absorbed Doses and Solvents

Three types of solvent were used, viz. cyclohexene, butanol and 1,4-Dioxane as a grafting media. It can be observed that the VIm could not be grafted onto PVDF film directly in cyclohexene solvent (see Table 1). No, or minimal grafting VIm onto PVDF at absorbed dose from 20 to 80 kGy, but only a few per cent (0.32 wt. %) occurs at 100 kGy. However, in the butanol solution, the grafting process occurred in all irradiation doses but the amount of grafted VIm monomer onto PVDF in the butanol solution was too small with less than 1.0 wt.%. In 1,4-dioxane, the VIm monomer was not grafted at 20 kGy, but the grafting process seems to occur at absorbed doses 40 and 60 kGy with DG 14.32 and 15.06 wt.%, respectively. However, unexpected results of samples were found to reduce in weight at absorbed dose 80 to 100 kGy. Therefore, it could be inferred that free radicals produced via scission may have reacted and grafted together with monomer to form a homopolymer. Thus, the reactive site in the polymer substrates has seemed 'ungraft' to the PVDF backbone, and it might not initiate grafting due to the high concentration of monomer. High concentrations of monomer possibly speed up the formation of homopolymer rather than tethering the monomer onto a polymer substrate. It was thought that excessive monomer and high doses of radiation sometimes might be considered to reduce the weight of PVDF trunks. Therefore, when PVDF film was immersed in different solvents consisting of VIm monomer, the homo PVIm was the most abundantly formed during the mutual irradiation by γ-rays.

Table 1 The effect of irradiation absorbed doses on VIm monomer dissolved in different solvents without metal ions (iron (II), FeSo4.7H_2O)

Simultaneous irradiation doses (kGy)	DG (wt.%) VIm in Cyclohaxene	DG (wt.%) VIm in Butanol	DG (wt.%) VIm in 1,4-Dioxane
20	0	0.03	0.00
40	0	0.05	14.32
60	0	0.03	15.06
80	0	0.06	-67.57
100	0.32	0.71	-18.80

A small amount of ferrous salt as a reducing agent was introduced (see Table 2) into all types of solvents. In general, it can be seen that the DG increased quickly at 20 to 60 kGy absorbed doses and remarkably decreased at high energy absorbed doses (80 to 100 kGy) for all types of solvent. The highest DG obtained is up to 85.52 wt.% when VIm dissolved in cyclohexene, 27.51 wt% in butanol and 145.93 wt.% when dissolved in 1,4-dioxane respectively at 60 kGy doses. However, the result of DG of VIm dissolved in butanol shows little significance since the variation of absorbed doses does not depict any significant trend with the DG of VIm onto PVDF trunks. Hence, the DG results of absorbed doses of 60 kGy are only reasonable for cyclohexene and 1,4-Dioxane.

The results also show that at higher absorbed doses (80 to 100 kGy), these doses are not ideal for grafting VIm onto PVDF films. The copolymerization might be due to the interactions between the irradiation-induced free radicals and their recombination, which significantly reduced the number of active sites for graft polymerization and resulted in the decline of DG. Furthermore, in high absorbed doses, γ-rays initiate speed homopolymerization rather than grafting onto the polymer backbone. Thus, at high monomer concentration, γ-rays create free radicals in the monomer at the first stage and undergo recombination or homopolymerization. In the next step, a few radicals are available to start copolymerization onto PVDF matrix base films. Thus, it could be concluded that at a high absorbed dose of above 80 kGy and high monomer concentration, these conditions are not suitable for grafting VIm monomer onto the PVDF backbone. It could increase producing homo PVIm without any metal ions as an initiator or reducing agent during simultaneous irradiation of γ-rays. In most cases, the grafting process of VIm onto PVDF is not sufficient without ferrous salt. Then, 1,4-Dioxane is the best solvent for the grafting mechanism with a DG of 145.93 wt.% and 60 kGy is the best irradiation dose exposed to the samples.

Table 2 The effect of irradiation absorbed doses on VIm monomer dissolved in different solvents without metal ions (iron (II), FeSo4.7H_2O)

Simultaneous irradiation doses (kGy)	DG (wt.%) VIm in Cyclohaxene	DG (wt.%) VIm in Butanol	DG (wt.%) VIm in 1,4-Dioxane
20	3.53	27.51	14.06
40	9.83	18.05	123.73
60	85.52	22.06	145.93
80	47.56	27.01	37.46
100	64.27	26.13	28.29

Grafting solution composition: VIm/solvent = 1/1 (v/v) containing 0.0025 M of $FeSO_4.7H_2O$; reaction temperature: 60°C at dose rate 0.0364 kGy/min.

3.2 Effect of Monomer

The effect of monomer composition on the PVDF-g-P1VIm has been studied by mass analysis using samples that were irradiated at the second stage (fixed at 60 kGy). Fig. 1 shows the impact of VIm concentration (0.5, 1.0, 2.0, and 3.0 M) onto PVDF backbone containing iron (II) or ferrous with concentration 0.0025M after irradiation with γ-ray at 60 kGy. The degree of grafting of the monomer reached its maximum grafting yield up to 46.7 % at 3.0 M at 60 kGy of absorbed dose. The degree of grafting yield starts to saturate at a high concentration of VIm due to the free radical scavenging or rapid formation of homopolymer at a high concentration of VIm [32]. Furthermore, the levelling off grafting yield may be attributed to the condition that affects the degree of saturation achieved between in solution and excited bonding of the PVDF backbone. Self-polymerization continues to form homopoly(VIm), which includes a diffusion barrier on the PVDF surface, as reflected in the grafting curve in the concentration of VIm . Similar findings were observed in the graft copolymerization of N-Vinylimidazole onto Poly (ethylene terephthalate) fibers [33]. In addition, VIm is a retarding agent by dissipation of the radiation energy forming a stable state that prevents the free radical formation responsible for the initiation of grafting sites. Therefore, the monomer solution containing excess VIm hinders the grafting of the comonomer onto the polymer substrate [34,35].

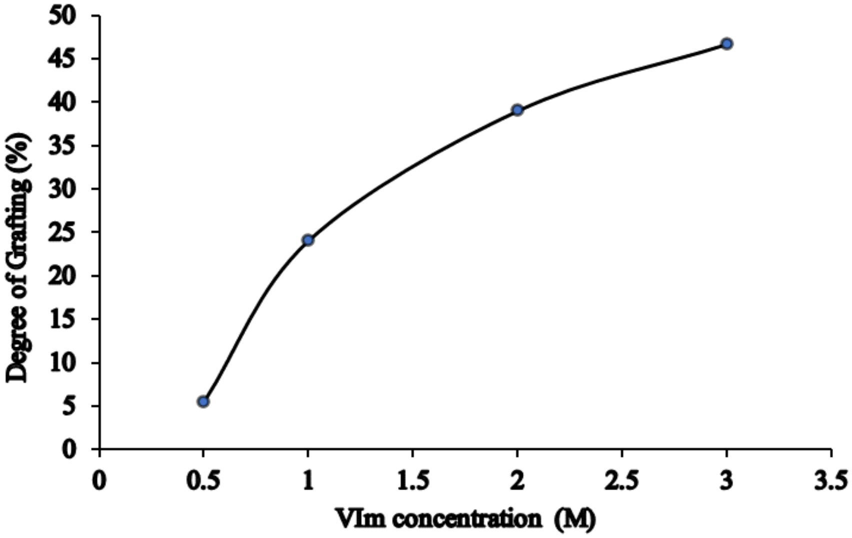

Figure 1. Effect of VIm concentration on grafting yield of PVDF backbone at 60 kGy of absorbed dose.

3.3 Effect of Iron (II) Sulfate Heptahydrate

Since the absorbed dose delivered was best at 60 kGy, the next samples were irradiated at different Iron (II) concentrations at a constant amount of VIm (2.0 M) in a Dioxane solution. Results of DG values for samples with different Iron (II) concentrations after being exposed to γ-rays at 60 kGy are tabulated in Table 3. Results from Table 3 indicate that the DG values of the VIm monomer onto the PVDF main chain are influenced by the concentration of iron (II) that existed in the solution. Different numbers of DG percentages are obtained below 100%. However, only a few samples have shown more than 100% of DG. Iron (II) or Fe (II) added to a gamma-irradiated solution can give rise to the Fenton reaction [36]. The radiation can induce a Fenton reaction, which eventually produces oxidizing radicals (•OH, H_2O_2, $HO^{\bullet}_2$ and O_2) that can promote grafting yield subsequently with the chemical compound in the solution. Iron (II) concentration of 0.0025M was the best for monomer attachment onto PVDF trunks immersed in Dioxane containing 1-Vinylimidazole.

The grafting process between polymer and monomer using radiation-induced grafting can occur if the Iron (II) exists in solution mixtures. The VIm and PVDF backbone are broken by γ-rays that induce scission of the chemical bond. Here, Iron (II) was used to initiate grafting that also acted as coordination chemistry between excited PVDF and VIm. The •OH radicals can attack the heterocyclic ring and aromatic ring (N–H) of the VIm molecule. Because of the strong negative charge between the nitrogen atom and aromatic ring, the N–H bond was easily attacked, particularly by the unsaturated bond of the VIm monomer, which underwent a series of reactions [36]. These reactions can form a longer poly –VIm onto the side chain of the PVDF backbone structure. This result provides the mechanism of longer formation DG of the side chain (PVIm) onto PVDF due to the advanced oxidation processes (AOPs) [37]. AOPs are commonly used for the Fenton reaction, in which hydrogen peroxide can be produced during radiation. Which can be split into hydroxyl radicals (•OH) by reacting with iron (II), Fe^{2+}. Therefore, during the γ-irradiation process, if Fe^{2+} exist in the solution, it could be formed more reactive of hydroxyl (•OH) and ferric ion (Fe^{3+}). As a result, the VIm monomer grafting onto PVDF can be interpreted by coordinating Fe^{2+} or Fe^{3+} [38]. Based on the discussion mentioned above, the possibility of the entire mechanisms for Fe (II) irradiation in the VIm solution containing PVDF precursor film for the Fenton reaction is proposed as in the following equations (8) to (12).

Table 3 DG in various amounts of Iron (II) and silica irradiated at 60 kGy of absorbed dose in dioxane solution

Samples No.	Iron (II) concentration, M	Weight before irradiation (w_b), g	Weight after irradiation (w_a), g	Degree of grafting (DG) $\frac{(w_a - w_b)}{w_b} \times 100\%$
1	0.0025	0.0236	0.0458	94.07
2	0.005	0.0298	0.0548	83.89
3	0.01	0.0341	0.0645	89.15*
4	0.05	0.0389	0.0700	79.95
5	0.1	0.0389	0.0765	96.66
6	0.0025	0.0226	0.0565	150.00
7	0.005	0.0313	0.0632	101.92
8	0.01	0.0356	0.0566	58.99*
9	0.05	0.0382	0.0853	123.30*
10	0.1	0.0397	0.0561	41.31*

* Selected for conductivity study

$$\mathbf{VIm\ solution}\ \overrightarrow{\gamma - \mathbf{rays}}\ \mathbf{H_2O_2, \bullet OH, OH_2^{\bullet}} \tag{8}$$

$$\mathbf{H_2O_2, \bullet OH, HO_2^{\bullet} + Fe^{2+} \rightarrow Fe^{3+}} \tag{9}$$

$$\mathbf{Fe^{3+} + VIm^{\bullet} \rightarrow Fe(III)VIm^{\circ}} \tag{10}$$

$$\mathbf{Fe^{3+} + PVDF^{\bullet} \rightarrow Fe(III)PVDF^{\circ}} \tag{11}$$

$$\mathbf{Fe(III)VIm^{\circ} + Fe(III)PVDF^{\circ} \rightarrow PVDF^{\circ} \ldots VIm^{\circ}} \tag{12}$$

Since the grafting (percentage) results obtained could be considered high; therefore, it could be inferred that VIm grafted onto PVDF main chain is a repeated monomer of VIm. Thus, it is thought that VIm grafted onto PVDF backbone could be attributed to the longer monomer VIm to form poly(1-vinylimidazole) side chain. The product of the membrane can be written as PVDF-g-P1VIm. The whole mechanism proved that the effect of Fe^{2+} addition on VIm solution has improved significantly grafting monomer onto polymer by radiation-induced of γ-rays to form

PVDF-g-P1VIm products. Therefore, this preparation of grafting indicates that the 1,4 Dioxane solution with 2.0 M concentration of VIm is the best media of solution to maximize the grafting of monomer (VIm) onto the polymer backbone of PVDF.

3.4 Effect of Fe^{2+}/Fe^{3} Ions Complexations Initiate Radiation-Induced Grafting

Iron is divided into two oxidation states: ferrous (Fe^{2+}) and ferric (Fe^{3+}), both of which are classified as ionic compounds with unique metal ion content. The oxidation of ferrous ions Fe (II) to ferric ions Fe (III) in an aqueous solution of sulfuric acid irradiated by ionizing radiation has been extensively studied [39]. These ions are essential as an initiator during the modification of polymeric properties via ionizing radiation. Then, the coordination number of imidazole groups of VIm/PVIm to a metal ion has four coordination for Fe^{2+}/Fe^{3+} ion complexes in aqueous solution [40]. Complexation equilibrium of Fe^{2+}/Fe^{3+} ions with VIm/PVIm could promote the grafting mechanism of VIm onto PVDF through radiation of γ-rays. VIm/PVIm is a polymeric ligand containing functional groups that are usually used to bind transition metal ions [41] PVIm/Cu^{2+}[42] and PVIm/Fe^{2+} [43]. The concentration level of Fe^{2+} was selected around 0.0025 M to fulfil the grafting mechanism between pristine PVDF base polymer and VIm monomer side chain. The existence of Fe^{2+}/Fe^{3+} plays a major role in grafting VIm onto PVDF to form a membrane called "PVDF-g-P1VIm". Fe^{2+}/Fe^{3+} ions are coordinated with the excited state of the PVDF* (activated polymer) and VIm* (activated monomer) before the grafting mechanism occurred. Adding inhibitors such as Fe2+ salts can suppress unnecessary side reactions and improve grafting efficiency [44]. Without this metal ion, the grafting mechanism could not be carried out successfully.

3.5 Degree of Swelling

The presence of hydrophilic and protonic groups at the side chain of the polymer backbone facilitates the swelling behavior of polymeric membranes. Table 4 shows that when the PVDF-g-P1VIm(H^+) membrane swells due to its affinity for water, the number of ionizable groups in the system increases proportionally, as do the degree of swelling (DS) and the diameter of the membrane. Fig. 3 indicates that the degree of swelling is slightly increased exponential with the degree of grafting. For example, at a low grafting level of DG41.4 %, it swells in the water by approximately 8.7 %. Following that, samples DG58.9% and DG89.2 % swelled to 13.2 and 18.0%, respectively. The swelling of the grafted membrane increased to approximately 39% at a high level of VIm grafting for sample DG123 %. This study, therefore, indicates that the grafting level has swollen the samples in water from the range of 8 to 40%. However, the membranes swelling less than 40% is considered sufficient to maintain the mechanical strength of the membranes. Swelled grafting membranes are correlated with diameter rise when the degree of grafting increased.

A graph of DG versus DS is plotted to demonstrate the relationship between DG and DS parameters. It is discovered that there is an exponent correlation between DG and DS as shown in Fig. 2. This implies that as DG increases, the water content in the membrane increases exponentially due to the hydrophilic nature of VIm to water.

Table 4 Effect of various grafting percentages of PVDF-g-P1VIm on the degree of swelling

Degree of Grafting (%), DG	Diameter before grafting (cm)	Diameter after grafting (cm)	Diameter in water (cm) (immersed 3 times in water)	Average diameter (cm)	Degree of Swelling (%), DS
41.4	2.0	2.30	2.50, 2.50, & 2.50	2.50	8.7
58.9	2.0	2.40	2.80, 2.65, & 2.70	2.70	13.2
89.2	2.0	2.50	2.90, 3.00, & 2.95	2.95	18.0
123.3	2.0	2.75	3.48, 4.00, & 4.00	3.80	39.2

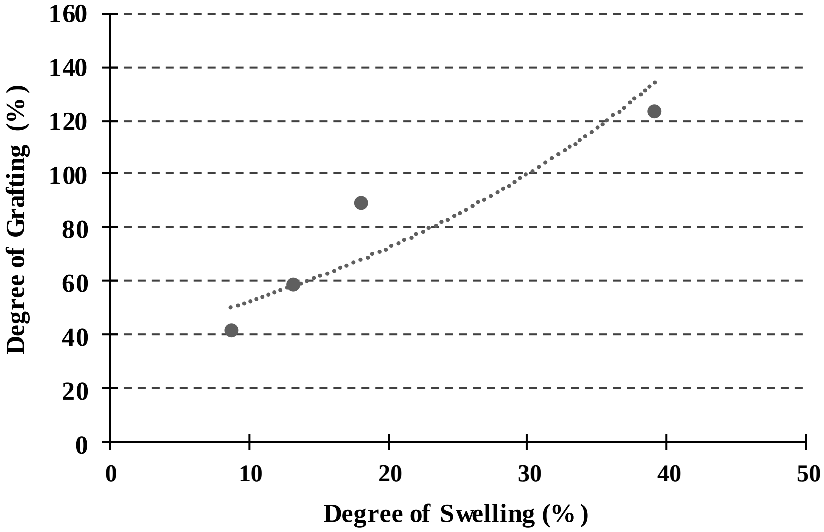

Figure 2. Correlation between DG and DS

3.6 Water Uptake

Water uptake (WU) can be defined as the weight ratio of water absorbed by the grafted membrane to the dried membrane. Fig. 3 displays DG of the PVDF-co-P1VIm *vs.* WU. It is seen that the water uptake increases with DG due to the growing number of ion exchange sites in the membrane, building the membrane more hydrophilic. The WU is increased exponentially with the DG. The increase of grafted VIm monomer onto PVDF trunks through radiation-induced grafting is aligned with increased water uptake, IEC, and conductivity study. This study, therefore, indicates that the grafting level gained a high-water level in yield membranes in the range of 16 to 78%. However, in samples that reach the highest degree of grafting (e.g., DG123.3%), they have achieved and exceeded bulk grafting, causing that water uptake could not occur due to graft distribution being saturated. P1VIm in the PVDF side chain has been saturated, resulting in excessive homopolymerization to form a longer side chain capable of absorbing more water contained in the PVDF-g-P1VIm membrane.

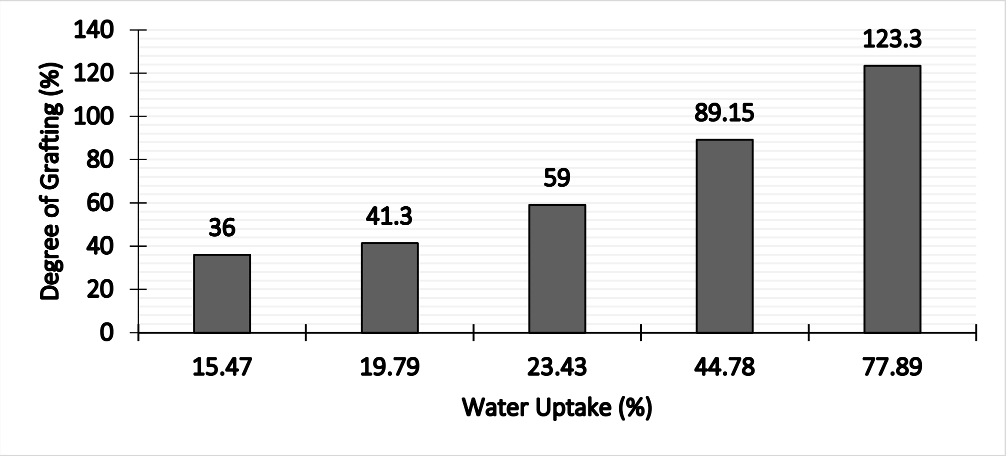

Figure 3. Effect of water uptake on the various degree of grafting for protonated PVDF-g-P1VIm membranes

3.7 Ion Exchange Capacity and Degree of Protonation

IEC is the site for ions to exchange between proton and sodium ion when the protonated membrane titrated with sodium chloride during acid-base titration. The grafting of 1-vinylimidazole monomer onto PVDF can be classified as an ion exchange membrane with polar monomer behavior.

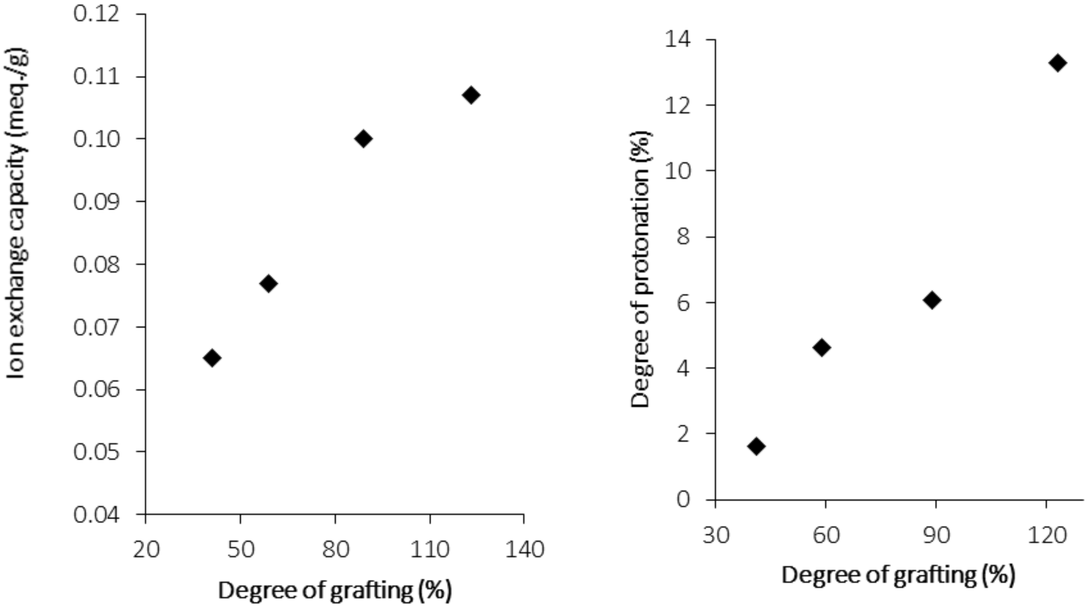

Figure 4. Correlations of IEC and DP with DG

The grafting of polar vinyl monomer such as Vinylimidazole directly confers cationic character to the polymer substrate, further modified by complexation in acid sulfuric [45,46]. Thus, the complexation of the PVDF-g-P1VIm membrane immersed in sulfuric acid displays ion exchange properties owing to fix protonic sites to the PVDF-g-P1VIm membrane. The percentage degree of protonation (DP) of protonated PVDF-g-P1VIm can be used to calculate the number of protonic species containing membranes. DP is analogous to acid content when the PVDF-g-P1VIm membranes immersed for 24 hours in 0.2 M acid sulfuric. Fig. 4 illustrates the relationship between the DP, IEC, and DG of protonated PVDF-g-P1VIm membranes.

3.8 FTIR Spectrum of the PVDF, 1-Vinylimidazole and PVDF-g-P1VIm

PVDF is a semicrystalline polymer having a chemical composition of C, H, and F that can be expected to be infrared active. Fig. 5 (a) and (b) depict the molecular structure of PVDF and 1-Vinylimidazole respectively. The repeating unit in PVDF molecular structure is $–CH_2$-CF_2-. In addition, an unirradiated 1-Vinylimidazole (VIm) with the molecular structure of heterocyclic 5-membered ring ($C_2H_6N_2$).

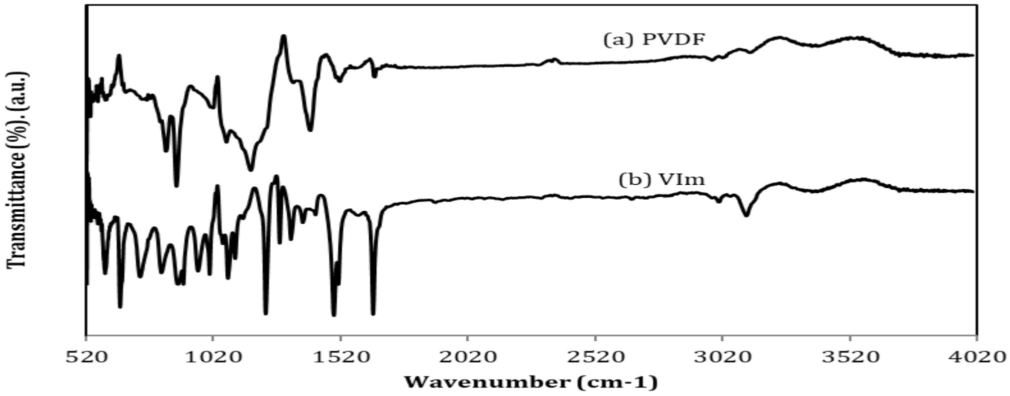

Figure 5. FTIR spectrum of (a) PVDF and (b) VIm sample showing transmittance (T%) as a function of wavenumber (cm^{-1}) for the range 4020-520 cm^{-}

The focus of vibrational spectroscopic characterization of PVDF is H-C-H. The H-C-H chemical bond is the weakest bonding compared to other chemical structures such as F-C-F and C-C-C bond via slow energy plasma treatment [47]. VIm is a monomer with a chemical composition of C, H, N and $C_5H_6N_2$. The main target of vibrational spectroscopic characterization of VIm monomer and its polymerization form of poly(1-Vinylimidazole) (PVIm) is H-C-H. The H-C-H structure is the target molecular structure in IR study due to its similarity in chemical structure with PVDF. Therefore, careful infrared spectroscopy of C-H using an FTIR spectrometer must be carried out to understand the molecular bonding between VIm (monomer) and PVDF (primary polymer) and its grafting mechanism via γ-rays induced grafting.

Effect of ionizing radiation onto hydrocarbon polymer usually is focused on C-H, C-C and C-F bonds of studying molecular bonding structure and functional group analysis [48,49]. In general, fluoropolymers backbone such as PVDF is formed of carbon-carbon (C-C) bonds and carbon-fluorine (C-F) bonds which are crystalline plastics and are powerful bonds with energy for one molecule 607 kJ.mol^{-1} and 552 kJ.mol^{-1} respectively [50]. In addition, the high electronegativity of the fluorine atoms via C-F bonds could result in low polarizability that giving fluorocarbon materials high thermal and chemical stability [51,52]. However, the C-H bonding is considered weak hydrogen bonds and the most widely studied [53,54]. Therefore, the C-H bond is significantly more vulnerable than the C-F bond making it more susceptible to scission by radiation [55]. Since the C-H bonds are weak hydrogen bonding, cleavage by radiation of γ-rays was investigated. IR spectra could be analyzed to verify the shifted and not shifted peaks of the molecular structure. Furthermore, the IR spectrum could also confirm the formation of a new bonding design which peaked after grafting of the polymer and monomer.

3.9 C-H and N-H Structure

The chemical structure was evaluated of C-H and N-H in IR spectra in a specific wavenumber. The C-H and N-H structures could provide vital information to confirm the grafting mechanism that occurred between PVDF and VIm and protonation by acid in PVDF-g-P1VIm membrane. Fig. 6 depicts the structural characterization of the pristine PVDF, PVDF-g-P1VIm, acid form of PVDF-g-P1VIm membranes characterized by FTIR spectroscopy in the region between 1500 – 1700 cm^{-1}. These are the molecular structure of N-H bending vibration around 1541 and 1578 cm^{-1} (dash lines). Pristine PVDF and PVDF-g-P1VDF show medium intensities, as depicted in Fig. 6 (a) and (b). However, this intensity peak is observed to increase and broaden after protonation in Fig. 6 (c). Some peaks in N-H increased due to acid sulfuric (H^{+}) and imidazole interaction. Characteristics of the broadening and increasing peak of the FTIR spectrum of PVDF-g-P1VIm(H^{+}) confirmed PVDF and VIm had been functionalized with a proton-conducting in the membrane.

Fig. 7 (i) shows the FTIR spectra of (a) pristine PVDF, (b) PVDF-g-P1VIm, and (c) protonated PVDF-g-P1VIm in a region between 2800 and 3200 cm^{-1}. The C-H and N-H region spectra and some peaks might overlap between C-H and N-H in this region. They yield two C-H stretching peaks at 2929 cm^{-1} and 2975 cm^{-1} for pristine PVDF, PVDF-g-P1VIm, and protonated PVDF-g-P1VIm respectively. These peaks are seemly not shifted to other wavenumbers. However, the intensity of peak increased and shifted to the right for the grafted PVDF and protonated PVDF-co-VIm. Thus, it can be inferred that the increases in the intensity of the C-H peak are due to the occurrence of grafting and complexation with VIm and acid, respectively.

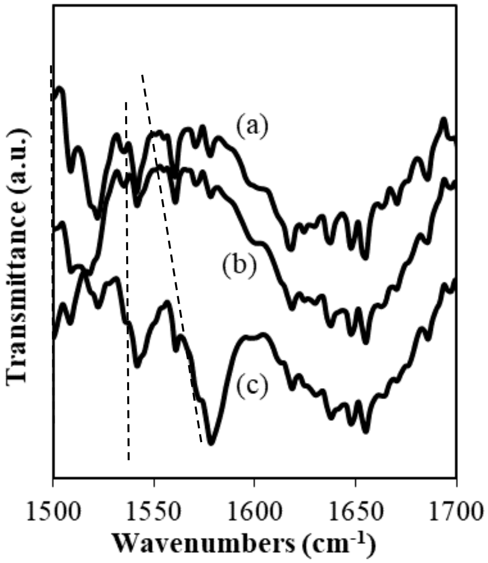

Figure. 6. FTIR spectra of (a) pristine PVDF, (b) PVDF-g-P1VIm, and (c) protonated PVDF-g-P1VIm in a region between 1500 and 1700 cm^{-1}.

Fig. 7 (ii) shows the structural characterization of the pristine PVDF, PVDF-g-P1VIm, protonated PVDF-g-P1VIm membranes in the region between 3000 and 3700 cm^{-1} characterized by FTIR spectroscopy. The pristine PVDF exhibits C-H stretching vibrations at 3027 cm^{-1}. Upon the grafting of VIm, the C-H band at 3027 cm^{-1} is observed to shift at higher wavenumbers. This peak shifts at 3117 cm^{-1} for the grafted PVDF-g-P1VIm and shifts at 3129 cm^{-1} for the protonated PVDF-g-P1VIm with sulfuric acid. These indicate that a strong interaction between imidazole group and PVDF as well as the occurrence of complexation between imidazole group and acid. Thus, the C-H shift validates the interaction between the VIm monomer and protonic group of acid. The other N-H stretching vibrations band occurs in the region 3000 to 3700 cm^{-1}. The broad peak of N-H bands is observed near 3400 cm^{-1}. N-H band is observed to shift from 3409 cm^{-1} to 3394 cm^{-1} for grafted PVDF-g-P1VIm membrane, and it is turned to 3398 cm^{-1} for the acidic PVDF-g-P1VIm (H$^+$) membranes. These moved bands to lower wavenumbers may be attributed to hydrogen bonding between N−H of 1-vinylimidazole (VIm) and protonic species N−H$^+$ from acid sulfuric.

In addition, there are unchanged of N-H or C-H absorption bands for pristine PVDF around 3100 to 3150 cm^{-1}. Then, the N-H regions have appeared at the right of 3000 cm^{-1} of aromatic rings for PVDF-g-P1VIm and acidic form of PVDF-g-P1VIm (H$^+$), which confirms a new peak of 3105 cm^{-1} has existed after being grafted with 1-vinyilimidazole. Meanwhile, this peak is observed to broaden and shifted at 3117 cm^{-1} in the acidic PVDF-g-P1VIm membrane. The broad rise in this region proves that imidazole and protonic species have a strong interaction [56,57]. With the presence of N-H interaction, it can be summarized that the 'protonated' imidazole group occurred and functionalized. It suggested that the acid condition caused a protonation of PVDF-g-P1VIm membrane. In other words, the properties of the membrane after complexation with acid sulfuric would form PVDF-g-P1VIm (H$^+$) in which this membrane behaves for a protonic carrier.

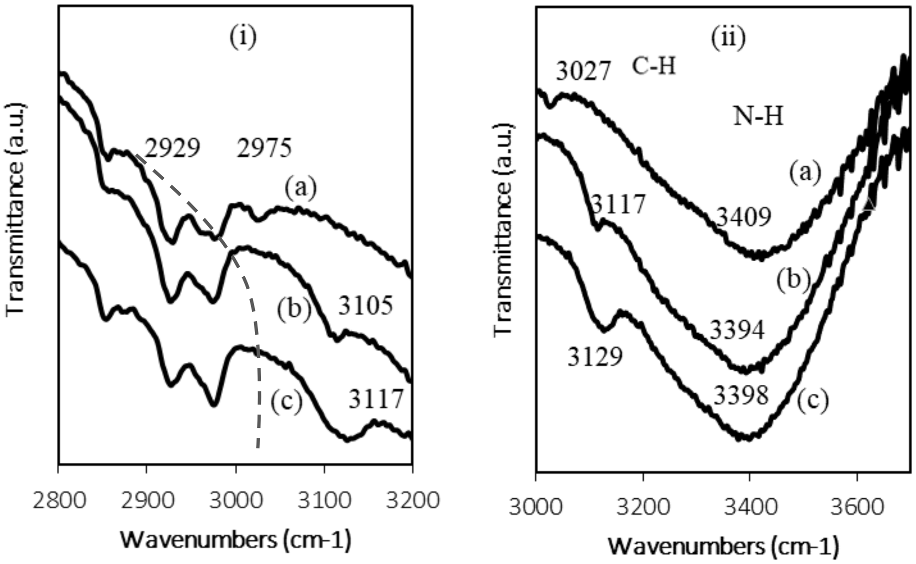

Figure 7. FTIR spectra of (a) pristine PVDF, (b) PVDF-g-P1VIm, and (c) protonated PVDF-g-P1VIm in a region between (i) 2800 and 3200 & (ii) 3000 and 3700 cm^{-1}

1.1 Protonated of PVDF-g-P1VIm membrane

In previous work, Li and coworkers reported that the N-H stretching of the protonated poly(1-vinylimidazole) had appeared gradually at vibration bands of 2480 and 2610 cm^{-1} [58]. Their finding was in line with that peaks of study C-N···H$^+$ band were observed at around 2634, or 2638 or 2636 cm^{-1} (for different samples). The C-N···H$^+$ chemical weak bonding interaction, which tethered functional imidazole, was protonated the PVDF-g-P1VIm into PVDF-g-P1VIm-H$^+$ membranes after complexion in H_2SO_4.

The band intensity at these peaks was weak indicates that the molecular interaction between N and H$^+$ in the C-N-H$^+$ (in a heterocyclic ring of imidazole) is considered a weak hydrogen bonding. In other words, the C-N···H$^+$ is ionic interaction. The weak hydrogen-proton bonding could be speculated that proton efficiently conducted loosely in imidazole ring. These conditions provide the PVDF-g-P1VIm-H$^+$ the membrane as a promising proton conductor for developing a new proton exchange membrane. This finding is consistent with some works that the imidazole species easily form protonated conditions when complexed with acid [59–62]. Thus, it could infer that the imidazole functional group in the side chain of PVDF is protonated by acid sulfuric.

1.2 Transference Number

Table 5 show the transference number (TN) non-protonated and protonated membrane with the concentration of 1-Vinylimidazole. The TN of the non-protonated membrane is 0.438. This value indicates that the non-protonated membrane is not entirely or partially ionic. However, the increase in ionic current with time in both grafted membranes follows a similar pattern, and the ionic transference number is close to 1 (0.993 and 0.991). The TN result shows that the charge carriers are ionic conductors. Ionic conductor implies that the conductivity of the PVDF-g-P1VIm(H$^+$) membranes was primarily due to ions, with electrons playing a minor role.

Table 5 The polar ization current as function of time protonated (a) PVDF-g-P1VIm (2.0 M) and (b) PVDF-g-P1VMm (1.0 M) respectively at room temperature

Membrane composition	Total current (I_T), A	Steady-state current (I_s), A	Ionic Transference number (t_{ion})
Non-protonated membrane	3.1 x 10^{-9}	1.74 x 10^{-9}	0.438
Protonated (1.0 M)	0.000475	3.2 x 10^{-6}	0.993
Protonated (2.0 M)	0.000661	6.1 x 10^{-6}	0.991

The results of transport number for various DG of the samples are tabulated in Table 6. The TN for the system was measured to be 0.84 up to 0.92 for different DG of protonated membranes indicating that the conductor species in the electrolyte system is predominantly ionic and electronic contribution to the electrical transport is negligibly very small. These results also demonstrate that, when the DG increased the ionic TN measurably increased.

Table 6 Transference number of different DG of protonated PVDF-g-P1VIm(H^+)

Degree of grafting (%)	**Total current (I_T), A**	**Steady-state current (I_s), A**	**Ionic transference number (t_{ion})**
58.9	2.92×10^{-8}	4.70×10^{-9}	0.84
89.2	3.28×10^{-8}	3.81×10^{-9}	0.88
123.3	5.60×10^{-8}	4.70×10^{-9}	0.92

1.3 Ionic Conductivity

Figure 8 depicts the variation of proton conductivity with different levels of VIm concentration at temperatures ranging from 293 to 373 K. At all temperatures and RH 80 % values, the conductivity of all membranes steadily increases with an increase in the concentration level.

The conductivity for all concentrations increases with rising temperature, as seen in the plot of log σ vs. 1000/T for 0.5 M, 1.0 M, 2.0 M, and 3.0 M of VIm concentrations. The log σ versus 1000/T curve is nearly linear, demonstrating that the conductivity is thermally assisted and that ionic conduction follows the Arrhenius law. However, with the exception of 0.5 M, the ionic conductivity of all samples increases dramatically at temperatures ranging from 323 to 333 K. The abrupt changes in conductivity indicate a phase transition in the grafted polymer membrane. Because of the VIm copolymer, the PVDF crystallinity transition could contribute to the phase transition around this temperature. The crystallinity transition that occurs at this temperature causes a substantial increase in ionic conductivity. A similar phase transition was observed in the PZT/PVDF-HFP composite study [63].

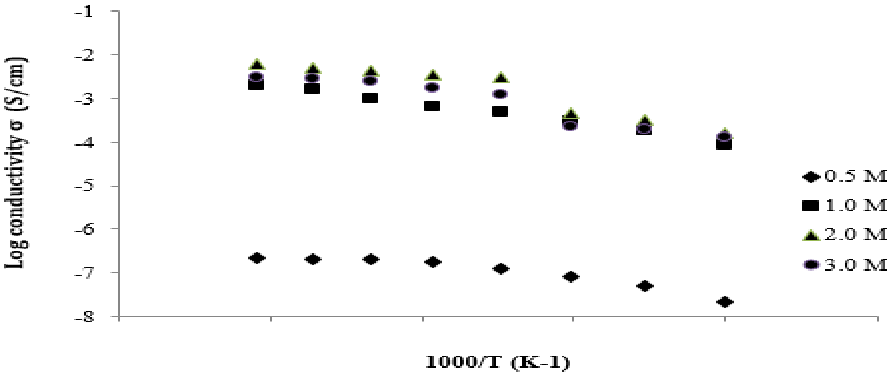

Figure 8. The conductivity study at different concentrations of VIm grafting onto PVDF backbone at 60 kGy of absorbed dosed (c) combination all concentration

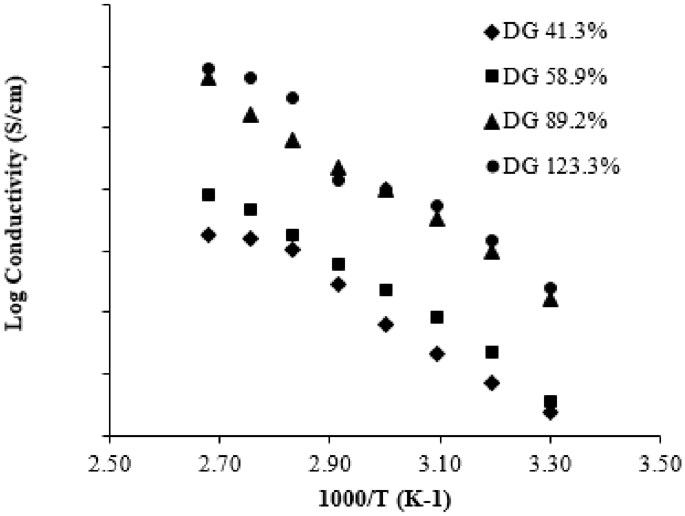

Figure 9. Proton conductivity of protonated PVDF-g-P1VIm membrane at varying DG is temperature dependent.

Fig.9 shows the conductivities of the protonated PVDF-g-P1VIm at various DG. After irradiation, the samples were evaluated using impedance spectroscopy to determine their conductivity to observe further the behavior based on the DG. For example, at the intermediate grafting level, DG 58.9%, the ionic conductivity pattern is more linear when the temperature level up from 273 to 373 K. It is seen to absolutely obey the Arrhenius law for the DG below 60%. However, above 80% grafting level, an abrupt change in ionic conductivity for temperature from 333 to 343 K occurred due to a change in the crystallization phase in this temperature region. The crystallization rate exhibits an inflection point at around 323-343 K, with higher rates in low temperatures, as reported by Pérez & coworkers [64]. The side chain of PVIm influenced the inflection area in crystallization temperature (T_c) of the primary chain PVDF. T_c caused an unprecedented rise in ionic conductivity, particularly at high grafting levels. Despite having a high grafting level of DG123.3%, the ionic conductivity performance is comparable to samples with DG89.2% and DG58.9%.

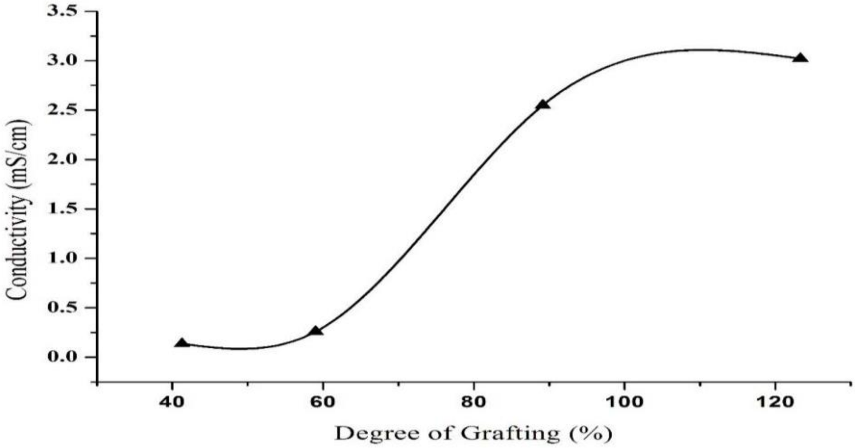

Figure 10. Correlation degree of grafting and conductivity

Fig. 10 shows correlation between DG and conductivity. Ionic conductivity of up to 10^{-4} Scm^{-1} has been observed in samples with grafting levels ranging from 30 to 60%. However, above the grafting level of 80%, there is a significant increase in ionic conductivity of up to 10^{-3} Scm^{-1}. At DG123.3%, the ionic conductivity is then found to be saturated. Since the ionic conductivity has reached 10^{-3} Scm^{-1}, grafting VIm onto PVDF matrices is sufficient to be prepared between 60 and 90% for future consideration. As a result, we expected that temperature and DG would affect the conductivity of protonated PVDF-g-P1VIm membranes.

3.13 Correlation Between DG, DS, DP, WU, IEC and Ionic Conductivity

The degree of grafting (DG) is related to with the degree of swelling (DS), water uptake (WU), degree of protonation (DP), ion exchange capacity (IEC) and ionic conductivity (σ). The relationships between the IEC, DP, and DG of PVDF-g-P1VIm protonic membranes are shown in Table 7. As the DG and DP increase, the IEC rises. Increases in the DG from 41 to 59 % result in an increase in the IEC from 0.065 to 0.077 meq.g^{-1}. The value range of these IEC produces ionic conductivity of up to 10^{-4} Scm^{-1}. However, high levels of graft (80 to 123.3 %) result in excellent ionic conductivity of up to 10^{-3} Scm^{-1}.

Table 7 Several degrees of grafting of the grafted PVDF membrane and correlation with IEC and conductivity

DG (wt.%)	DP (%)	IEC (meq./g)	Average IEC (meq./g)	σ (Scm^{-1}) at 373 K
41.3	1.62	0.065, 0.07, & 0.06	0.065	1.36×10^{-4}
59.0	4.62	0.08, 0.08, & 0.07	0.077	2.58×10^{-4}
89.15	6.07	0.07, 0.12, & 0.11	0.100	2.55×10^{-3}
123.3	13.3	0.12, 0.11, & 0.09	0.107	3.02×10^{-3}

Depending on the type of polymer sidechain grafted on the membrane surface, polymers with a higher grafting level could have a high or low IEC. IEC is always connected to DP and DG. IEC is a measure of ionic conductivity performance. Furthermore, the conductivity of the PVDF-g-P1VIm(H$^+$) membrane is highly dependent on IEC. The majority of samples consistently show a direct correlation between DG levels and IEC., but in some cases, the PVDF-g-P1VIm indicates a high level of DG that is not proportional to the IEC.

Thus, sample polymer matrix and monomer preparation, surface modification, and irradiation processing conditions might indeed contribute to different patterns of grafting level onto the polymer surface. These membranes have a marginal ionic conductivity of up to 10^{-3} Scm^{-1}. Ionic conductivity in this investigation was 10^{-3} Scm-1, which is quite comparable to Stewart & coworkers' findings [65] and Xu & Wang [66]. As the DG rose, the amount of poly(1-vinylimidazole) grafts in the PVDF matrix rose as well, which resulted in additional protonic groups being available linked to the imidazole group. Ionic conductivity was measured at 10^{-3} Scm^{-1} for IEC values obtained in the range of 0.100 to 0.107 meq.g^{-1}, as presented in Table 7. The DG measures the quantity of graft component attached to the base polymer. Using VIm as grafting monomers directly allows protonation of the aromatic ring to introduce ion exchange sites. In acidic conditions, unlike grafting styrene monomer onto polymer base, 1-vinylimidazole is easier to be protonated rather than sulfonated. The grafting imidazole leads to the appearance characteristics C-N$^+$-H or C=N$^+$-H (ring), which was proton bonding that contributed to form the polyelectrolyte and proton-conducting in the membranes [67].

There is a clear possibility that σ occasionally arises from DG, DS, WU, DP, and IEC. The conductivity of the ionic exchange membrane is largely influenced by these parameters in most cases. Therefore, the conductivity properties of the developed membrane are mostly determined by DG and IEC. Too much DG, on the other hand, is unlikely to have made a major contribution to greater ionic conductivity. This is because excessive grafting might not increase IEC but increase the side polymer, which tends to form a longer side chain. IEC can be a vital indicator for ionic transport that would affect and determine the ionic conductivity of the PVDF-g-P1VIm membranes. Additionally, a higher WU does not always equate to better conductivity. Despite the existence of total WU, conductivity is largely determined by IEC.

CONCLUSION

Utilizing a simultaneous radiation-induced grafting approach with γ-ray, PVDF as a polymer-based cografting with VIm as a monomer has been completed successfully. The concentration of monomers, iron (II) sulphate, and the absorbed dosage of γ-rays all affect the DG. The DS and WU for the PVDF-g-P1VIm were satisfactory. IEC values ranged from 0.100 to 0.107 meq.g-1 after protonation of the PVDF-g-P1VIm membranes in sulfuric acid. Information about the IEC is crucial since it serves as an indicator of the properties of proton conducting membranes. As a basis, the polymer membrane has a high IEC, and we may infer that it has a high level of protonic acid on PVDF-g-P1VIm membrane. In the membrane grafting system, 1-VIm, one of the important functional groups, can act as a proton acceptor. The addition of the protonated 1-VIm group to the copolymer considerably increases the conductivity of the material. The overall conductivity of the sulfuric acid-protonated PVDF-g-P1VIm membrane can approach 10^{-3} Scm^{-1}. Examining the effect of radiation on C-N-H and C-H structure, the IR investigation shows that VIm was successfully grafted onto the PVDF main chain. It was proven by IR analysis that PVDF and VIm were functionalized with proton conducting to create protonated membrane, which is the "important point" for building proton exchange membrane for fuel cell applications.

ACKNOWLEDGEMENTS

The authors would like to thank iMade research lab institute of science for their help and support in conducting this research and Universiti Teknologi MARA for financially supporting this work through Geran Lestari (600-RMC/MyRA 5/3/LESTARI (075/2020).

REFERENCES

[1] Caniani D, Caivano M, Mazzone G, Masi S, Mancini IM. Effect of site-specific conditions and operating parameters on the removal efficiency of petroleum-originating pollutants by using ozonation: A review. Science of The Total Environment 2021:149393. https://doi.org/10.1016/J.SCITOTENV.2021.149393.

[2] Deng J, Wang X, Wei Z, Wang L, Wang C, Chen Z. A review of NOx and SOx emission reduction technologies for marine diesel engines and the potential evaluation of liquefied natural gas fuelled vessels. Science of The Total Environment 2021;766:144319. https://doi.org/10.1016/J.SCITOTENV.2020.144319.

[3] Miyake J, Ogawa Y, Tanaka T, Ahn J, Oka K, Oyaizu K, et al. Rechargeable proton exchange membrane fuel cell containing an intrinsic hydrogen storage polymer. Commun Chem 2020;3. https://doi.org/10.1038/s42004-020-00384-z.

[4] Sasiwimonrit K, Chang W-C. Thermal management of high-temperature polymer electrolyte membrane fuel cells by using flattened heat pipes. Thermal Science 2020. https://doi.org/10.2298/tsci190324135s.

[5] Haque MA, Sulong AB, Majlan EH, Loh KS, Husaini T, Rosli R. Physiochemical characteristics of solid electrolyte membranes for high-temperature PEM fuel cell. Int J Electrochem Sci 2019;14. https://doi.org/10.20964/2019.01.26.

[6] Yang H, Zhang J, Yi B. Clean energy technology: materials, processes and devices for electrochemical energy conversion and storage. Frontiers in Energy 2017;11. https://doi.org/10.1007/s11708-017-0501-7.

[7] Elwan HA, Mamlouk M, Scott K. A review of proton exchange membranes based on protic ionic liquid/polymer blends for polymer electrolyte membrane fuel cells. J Power Sources 2021;484:229197. https://doi.org/10.1016/J.JPOWSOUR.2020.229197.

[8] Guo Z, Chen J, Byun JJ, Cai R, Perez-Page M, Sahoo M, et al. High-performance polymer electrolyte membranes incorporated with 2D silica nanosheets in high-temperature proton exchange membrane fuel cells. Journal of Energy Chemistry 2022;64:323–34. https://doi.org/10.1016/J.JECHEM.2021.04.061.

[9] Wang S, Jiang SP. Prospects of fuel cell technologies. Natl Sci Rev 2017;4:163–6. https://doi.org/10.1093/NSR/NWW099.

[10] Costa LMM. Effect of Solution Concentration on the Electrospray/Electrospinning Transition and on the Crystalline Phase of PVDF. Materials Sciences and Applications 2010;01:246–51. https://doi.org/10.4236/msa.2010.14036.

[11] Nasef M. Preparation and applications of ion exchange membranes by radiation-induced graft copolymerization of polar monomers onto non-polar films. Prog Polym Sci 2004;29:499–561. https://doi.org/10.1016/j.progpolymsci.2004.01.003.

[12] Tan Z, Fu C, Gao Y, Qian J, Li W, Wu X, et al. Modifications of Gamma poly (vinylidene fluoride) (γ-PVDF) films by high-energy electron beam irradiation. Radiation Physics and Chemistry 2018;153:258–68. https://doi.org/10.1016/J.RADPHYSCHEM.2018.06.051.

[13] Ashfaq A, Clochard MC, Coqueret X, Dispenza C, Driscoll MS, Ulański P, et al. Polymerization reactions and modifications of polymers by ionizing radiation. Polymers (Basel) 2020;12. https://doi.org/10.3390/polym12122877.

[14] Gürsel SA, Youcef H Ben, Wokaun A, Scherer GG. Influence of reaction parameters on grafting of styrene into poly(ethylene-alt-tetrafluoroethylene) films. Nucl Instrum Methods Phys Res B 2007;265:198–203. https://doi.org/http://dx.doi.org/10.1016/j.nimb.2007.08.050.

[15] Ferry M, Ngono-Ravache Y, Aymes-Chodur C, Clochard MC, Coqueret X, Cortella L, et al. Ionizing Radiation Effects in Polymers. Reference Module in Materials Science and Materials Engineering 2016. https://doi.org/10.1016/B978-0-12-803581-8.02095-6.

[16] Chen J, Li D, Koshikawa H, Asano M, Maekawa Y. Crosslinking and grafting of polyetheretherketone film by radiation techniques for application in fuel cells. J Memb Sci 2010;362:488–94. https://doi.org/http://dx.doi.org/10.1016/j.memsci.2010.07.012.

[17] Sherazi T a., Ahmad S, Kashmiri MA, Kim DS, Guiver MD. Radiation-induced grafting of styrene onto ultra-high molecular weight polyethylene powder for polymer electrolyte fuel cell application. J Memb Sci 2009;333:59–67. https://doi.org/10.1016/j.memsci.2009.01.052.

[18] F. Barakat M, M. El-Salmawy K, H. Zahran A, Barakat MF, El-Salmawy KM, Zahran AH. Radiation Induced Grafting of Acrylic Acid onto Viscose Rayon Fabrics and Its After-Effects. Open Journal of Polymer Chemistry 2016;06:27–42. https://doi.org/10.4236/ojpchem.2016.63004.

[19] Gupta B, Grover N, Singh H. Radiation grafting of acrylic acid onto poly(ethylene terephthalate) fabric. J Appl Polym Sci 2009;112. https://doi.org/10.1002/app.29546.

[20] Mohd Hidzir N, Mohd Radzali NA, Abdul Rahman I, Shamsudin SA. Gamma irradiation-induced grafting of 2-hydroxyethyl methacrylate (HEMA) onto ePTFE for implant applications. Nuclear Engineering and Technology 2020;52. https://doi.org/10.1016/j.net.2020.03.016.

[21] Lim SJ, Shin IH. Graft copolymerization of GMA and EDMA on PVDF to hydrophilic surface modification by electron beam irradiation. Nuclear Engineering and Technology 2020;52:373–80. https://doi.org/10.1016/J.NET.2019.07.018.

[22] Tekin N, Kadıncı E, Demirbaş Ö, Alkan M, Kara a., Doğan M. Surface properties of poly(vinylimidazole)-adsorbed expanded perlite. Microporous and Mesoporous Materials 2006;93:125–33. https://doi.org/10.1016/j.micromeso.2006.02.009.

[23] Pino-Ramos VH, Cedillo G, López-Barriguete E, Bucio E. Comonomer effect: Switching the lower critical solution temperature to upper critical solution temperature in thermo-pH sensitive binary graft copolymers. J Appl Polym Sci 2019;136. https://doi.org/10.1002/app.48170.

[24] Soresi B, Quartarone E, Mustarelli P, Magistris A, Chiodelli G. PVDF and P(VDF-HFP)-based proton exchange membranes. Solid State Ion 2004;166:383–9. https://doi.org/10.1016/j.ssi.2003.11.027.

[25] Turmanova S, Minchev M, Vassilev K, Danev G. Surface grafting polymerization of vinyl monomers on poly(tetrafluoroethylene) films by plasma treatment. Journal of Polymer Research 2008;15:309–18. https://doi.org/10.1007/s10965-007-9172-0.

[26] Mikulášova D, Citovický P. Redox polymerization systems for the preparation of grafted polypropylene . I . Grafting of polypropylene with styrene in the presence of triethylenetetramine metal chelates 1973;27:263–7.

[27] Rajabalizadeh Mojarrad N, Sadeghi S, Yarar Kaplan B, Güler E, Alkan Gürsel S. Metal-Salt Enhanced Grafting of Vinylpyridine and Vinylimidazole Monomer Combinations in Radiation Grafted Membranes for High-Temperature PEM Fuel Cells. ACS Appl Energy Mater 2020;3. https://doi.org/10.1021/acsaem.9b01777.

[28] Zahran MK. ORIGINAL ARTICLE HO HO. ARABIAN JOURNAL OF CHEMISTRY 2013. https://doi.org/10.1016/j.arabjc.2013.07.027.

[29] Chaudhari C V., Dubey K a., Bhardwaj YK, Kumar V, Goel NK, Sabharwal S. Radiation grafting of acrylonitrile on ethylene-propylene diene terpolymer rubber: Optimization of grafting parameters and oil resistance properties. J Radioanal Nucl Chem 2008;278:47–53. https://doi.org/10.1007/s10967-007-7152-9.

[30] Dessouki AM, Taher NH, El-Boohy HA. Radiation-induced graft polymermization of acrylamide onto poly(tetrafluoroethylene/ Hexaflouropropylene/vinylidene fluoride) (TFB) films. International Journal of Radiation Applications and Instrumentation Part 1990;36:371–5. https://doi.org/10.1016/1359-0197(90)90021-9.

[31] Baharin R, Ramli S, Hairaldin SZ, Ahmad R. Risk analysis and hazard identification at ALURTRON and MINTec-Sinagama. IOP Conf Ser Mater Sci Eng 2020;785. https://doi.org/10.1088/1757-899X/785/1/012050.

[32] Kumar A, Deka M, Banerjee S. Enhanced ionic conductivity in oxygen ion irradiated poly(vinylidene fluoride-hexafluoropropylene) based nanocomposite gel polymer electrolytes. Solid State Ion 2010;181:609–15. https://doi.org/10.1016/j.ssi.2010.02.027.

[33] Lilac WD, Lee S. Analysis of the solid phase copolymerization grafting process. Korean Journal of Chemical Engineering 1999;16:275–84. https://doi.org/10.1007/BF02707113.

[34] Ajji Z, Othman I, Rosiak JM. Production of hydrogel wound dressings using gamma radiation. Nucl Instrum Methods Phys Res B 2005;229:375–80. https://doi.org/10.1016/j.nimb.2004.12.135.

[35] Das T, Sengupta S, Jana A, Pal A, Roy I, Sardar S, et al. Graphene oxide grafted hyperbranched poly (vinyl imidazole) with ionic liquid components as a potential carbon dioxide scrubber. React Funct Polym 2020;146:104432. https://doi.org/10.1016/J.REACTFUNCTPOLYM.2019.104432.

[36] Liu J, Liu H, Li Y, Wang H. Probing the coordination properties of glutathione with transition metal ions (Cr2+, Mn2+, Fe2+, Co2+, Ni2+, Cu2+, Zn2+, Cd2+, Hg2+) by density functional theory. J Biol Phys 2014;40:313–23. https://doi.org/10.1007/s10867-014-9350-3.

[37] Zheng Z, Kang M, Wang C, Liu C, Grambow B, Duro L, et al. Influence of gamma irradiation on uranium determination by Arsenazo III in the presence of Fe(II)/Fe(III). Chemosphere 2014;107:373–8. https://doi.org/10.1016/j.chemosphere.2013.12.094.

[38] Marić I, Vujičić NŠ, Pustak A, Gotić M, Štefanić G, Grenèche JM, et al. Rheological, microstructural and thermal properties of magnetic poly(Ethylene oxide)/iron oxide nanocomposite hydrogels synthesized using a one-step gamma-irradiation method. Nanomaterials 2020;10:1–30. https://doi.org/10.3390/nano10091823.

[39] Baarli J, Borge P. The application of the ferrous-ferric system for routine measurements. Acta Radiol 1957;47:203–9. https://doi.org/10.3109/00016925709170888.

[40] Miyajima T, Nishimura H, Kodama H, Ishiguro S. On the complexation of Ag (I) and Cu (II) ions with poly (N -vinylimidazole) 1998;38:183–95.

[41] Tian AH, Kim J-Y, Shi JY, Kim K. Poly(1-vinylimidazole)/Pd-impregnated Nafion for direct methanol fuel cell applications. J Power Sources 2008;183:1–7. https://doi.org/10.1016/j.jpowsour.2008.04.085.

[42] Yuan S, Pehkonen SO, Liang B, Ting YP, Neoh KG, Kang ET. Poly(1-vinylimidazole) formation on copper surfaces via surface-initiated graft polymerization for corrosion protection. Corros Sci 2010;52:1958–68. https://doi.org/10.1016/j.corsci.2010.02.010.

[43] Meléndez-Ortiz HI, Alvarez-Lorenzo C, Burillo G, Magariños B, Concheiro A, Bucio E. Radiation-grafting of N-vinylimidazole onto silicone rubber for antimicrobial properties. Radiation Physics and Chemistry 2015;110:59–66. https://doi.org/10.1016/j.radphyschem.2015.01.025.

[44] Zhou T, Shao R, Chen S, He X, Qiao J, Zhang J. A review of radiation-grafted polymer electrolyte membranes for alkaline polymer electrolyte membrane fuel cells. J Power Sources 2015;293:946–75. https://doi.org/10.1016/j.jpowsour.2015.06.026.

[45] Nasef MM, Aly AA, Saidi H, Ahmad A. Optimization of reaction parameters of radiation induced grafting of 1-vinylimidazole onto poly(ethylene-co-tetraflouroethene) using response surface method. Radiation Physics and Chemistry 2011;80:1222–7.

[46] Vázquez E, Muro C, Illescas J, Burillo G, Hernández O, Rivera E. Obtainment and characterization of hydrophilic polysulfone membranes by N-vinylimidazole grafting induced by gamma irradiation. Polymers (Basel) 2020;12. https://doi.org/10.3390/POLYM12061284.

[47] Kormunda M, Ryšánek P, Hájková P, Štěpanovská E, Čapková P, Pavlík J. Effect of low energy plasma treatment on surface chemistry and phase composition of electrospun polyvinylidene fluoride membrane. Surfaces and Interfaces 2021;22. https://doi.org/10.1016/j.surfin.2020.100900.

[48] Li W, Zhu Y, Jiang limin, Wang P, Wang J. Study of irradiation effect on poly(vinylidene fluoride-trifluoroethylene) copolymers. J Mater Sci 2007;42:7186–90.

[49] Prasad SG, De A, De U. Structural and Optical Investigations of Radiation Damage in Transparent PET Polymer Films. Int J Spectrosc 2011;2011:1–7. https://doi.org/10.1155/2011/810936.

[50] Galante a. MS, Galante OL, Campos LL. Study on application of PTFE, FEP and PFA fluoropolymers on radiation dosimetry. Nucl Instrum Methods Phys Res A 2010;619:177–80. https://doi.org/10.1016/j.nima.2009.10.103.

[51] Ghosh S, Mukherjee R, Ghosh A, Mohanty AK, Banerjee S. Fluorinated Poly(Arylene Ether)s: Synthesis, Properties, and Applications. Handbook of Specialty Fluorinated Polymers: Preparation, Properties, and Applications 2015:11–96. https://doi.org/10.1016/B978-0-323-35792-0.00002-7.

[52] Souzy R, Ameduri B. Functional fluoropolymers for fuel cell membranes. Prog Polym Sci 2005;30:644–87. https://doi.org/http://dx.doi.org/10.1016/j.progpolymsci.2005.03.004.

[53] Kolesov BA. Hydrogen bonds: Raman spectroscopic study. Int J Mol Sci 2021;22. https://doi.org/10.3390/ijms22105380.

[54] Liu D, Lei W, Wang K, Bao G, Li F, Hao J, et al. Compression and probing C-H···I hydrogen bonds of iodoform under high pressure by X-ray diffraction and raman scattering. Journal of Physical Chemistry B 2009;113. https://doi.org/10.1021/jp900467z.

[55] Forsythe JS, Hill DJT. The radiation chemistry of fluoropolymers. Prog Polym Sci 2000;25:101–36. https://doi.org/10.1016/S0079-6700(00)00008-3.

[56] Celik SU, Bozkurt A. The synthesis and proton-conducting properties of the copolymers based on 1-vinyl-1,2,4-triazole and 2-acrylamido-2-methyl-1-propanesulfonic acid. Solid State Ion 2010;181:525–30. https://doi.org/DOI 10.1016/j.ssi.2010.02.019.

[57] He Y, Zhu B, Inoue Y. Hydrogen bonds in polymer blends. Prog Polym Sci 2004;29:1021–51. https://doi.org/10.1016/j.progpolymsci.2004.07.002.

[58] Li J, Zhang Y, Ping Z, Li M, Zhang Q. Synthesis and endotoxin removal properties of a novel affinity sorbent with poly(1-vinylimidazole) as the ligand. Process Biochemistry 2011;46:1462–8. https://doi.org/10.1016/j.procbio.2011.03.019.

[59] Andersson M, Hansson Ö, Öhrström L, Idström A, Nydén M. Vinylimidazole copolymers: coordination chemistry, solubility, and cross-linking as function of Cu2+ and Zn2+ complexation. Colloid Polym Sci 2011;289:1361–72. https://doi.org/10.1007/s00396-011-2461-5.

[60] Caner H, Yilmaz E, Yilmaz O. Synthesis, characterization and antibacterial activity of poly(N-vinylimidazole) grafted chitosan. Carbohydr Polym 2007;69:318–25.

[61] Danilovtseva EN, Annenkov V V, Mikhaleva AI, Trofimov BA. Copolymers of 1-vinylimidazole and acrylic acid for bioseparation. Polymer Science - Series A 2004;46:125–9.

[62] Goswami S, Dutta A. Measurement of ionic conductivity of poly (N-vinylimidazole) and its fluoroborate salt in solid state. Ionics (Kiel) 2011;17:627–32. https://doi.org/10.1007/s11581-011-0554-2.

[63] Malmonge LF, Malmonge JA, Sakamoto WK. Study of pyroelectric activity of PZT/PVDF-HFP composite. Materials Research 2003;6:469–73.

[64] Pérez E, Angulo I, Blázquez-Blázquez E, Cerrada ML. Characteristics of the non-isothermal and isothermal crystallization for the β polymorph in PVDF by fast scanning calorimetry. Polymers (Basel) 2020;12:1–17. https://doi.org/10.3390/polym12112708.

[65] Stewart KA, Singh M, Missan HPS. Novel PVdF-graft-VIm Based Nano-composite Polymer Electrolyte Membranes for Fuel Cell Applications. ECS Trans 2019;25:1459–68. https://doi.org/10.1149/1.3210702.

[66] Xu H, Wang A. 216th ECS Meeting, Abstract #3134, © The Electrochemical Society 2009:3134.

DOI: https://doi.org/10.15379/ijmst.v10i2.3243